Device

CellPress

Perspective

Intrinsically stretchable low-dimensional conductors for wearable organic light-emitting diodes

Huanyu Zhou,[1,3,4] Kwan-Nyeong Kim,[1,4] Min-Jun Sung,[1,4] Shin Jung Han,[1] and Tae-Woo Lee[1,2,*]

[1]Department of Materials Science and Engineering, Seoul National University, Seoul 08826, Republic of Korea

[2]School of Chemical and Biological Engineering, Institute of Engineering Research, Research Institute of Advanced Materials, Soft Foundry, Seoul National University, Seoul 08826, Republic of Korea

[3]BK21 PLUS SNU Materials Division for Educating Creative Global Leaders, Seoul National University, Seoul 08826, Republic of Korea

[4]These authors contributed equally

*Correspondence: twlees@snu.ac.kr

https://doi.org/10.1016/j.device.2023.100060

THE BIGGER PICTURE Significant advances in intrinsically stretchable conductors that use low-dimensional materials have propelled the development of stretchable displays. However, the design of intrinsically stretchable interconnects and transparent conductive electrodes that meet the requirements of high stretchability, high conductivity, and high transmittance poses a formidable challenge due to unavoidable trade-off relationships. Moreover, to increase the light-emitting efficiency of stretchable displays, charge-injection capability of the transparent conductive electrode must be optimized, and ways to achieve a tunable work function must be found. This perspective focuses on addressing the key challenges and providing solutions in the field of intrinsically stretchable low-dimensional conductors. Additionally, it provides valuable insights into the essential prerequisites of low-dimensional conductors for designing highly efficient, intrinsically stretchable organic light-emitting diodes suitable for wearable applications.

SUMMARY

Advances in wearable electronics have resulted in an increasing demand for stretchable conductors, which can serve as either interconnects or electrodes for intrinsically stretchable organic light-emitting diodes (ISOLEDs). Fulfilling this demand necessitates the development of stretchable conducting materials that exhibit high mechanical resilience and electrical conductivity. They can be achieved by incorporating low-dimensional materials within an elastomeric matrix. Moreover, maximizing the electroluminescence of ISOLEDs requires an increase in additional parameters such as optical transmittance and work function of stretchable electrodes. The simultaneous fulfillment of all these requirements presents a significant challenge in the quest for suitable stretchable conductors for ISOLEDs. This perspective focuses on key advances in intrinsically stretchable low-dimensional conductors and their applications as stretchable interconnects and electrodes for ISOLEDs. It also provides insights into prerequisites for designing highly efficient ISOLEDs for practical wearable devices.

INTRODUCTION

The proliferation of wearable and stretchable electronics has led to a significant expansion in the range and diversity of devices and their form factors.[1–4] The integration of multifunctional wearable electronics on human skin has unlocked their potential applications in body-area sensor networks.[5–7] On-skin displays represent the ultimate method to visualize information in real time.[8] However, due to the absence of established standards, design strategies, and processing techniques for stretchable materials and devices, the task of achieving a stretchable display that meets industrial standards remains a formidable challenge.

Materials used in stretchable displays must be capable of withstanding repeated tensile strain without significant loss of functional properties. The development of stretchable conductors is, therefore, crucial for the advancement of wearable electronics.[9,10] Two approaches to achieve this goal are available: (1) the use of geometric structures (e.g., buckling, serpentine, or island-bridge structures) to avoid tensile strain in active electronic device during deformation and (2) the use of intrinsically stretchable materials that can withstand

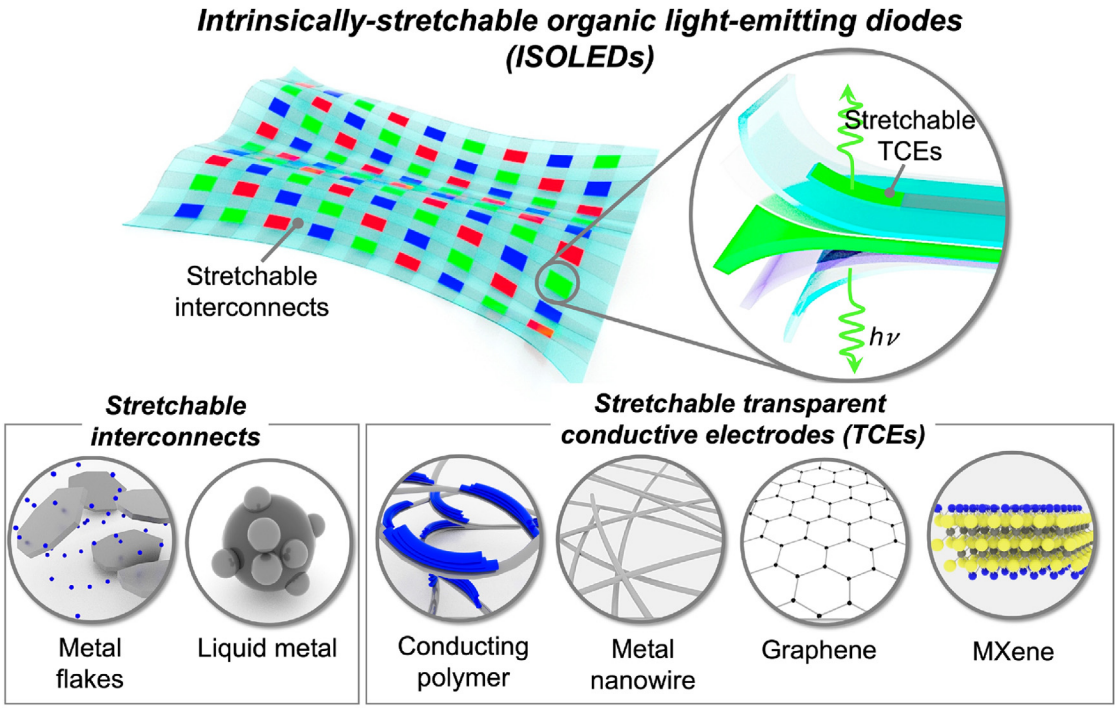

Figure 1. Schematic illustration of stretchable interconnects and transparent conductive electrodes for intrinsically stretchable organic light-emitting diodes (ISOLEDs) that use a variety of conducting materials

large mechanical deformation and thereby impart stretchability to the device. In 2017, Samsung Display unveiled a prototype active-matrix stretchable display that exploited a geometrically stretchable structure[11]; however, currently available intrinsically stretchable displays composed entirely of stretchable materials still do not meet industry standards. These deficiencies can be attributed to the absence of established standards, design strategies, and processing techniques for stretchable conductors that are suitable for use as both stretchable interconnects and transparent conductive electrodes (TCEs) in intrinsically stretchable organic light-emitting diodes (ISOLEDs) (Figure 1).

Conventional conductive materials, such as metal oxides, are inherently brittle, so they have limited applicability in intrinsically stretchable devices.[12–15] A method to mitigate the degradation caused by tensile strain ε involves using a stretchable interconnect composed of metal flakes or liquid-metal particles as conductive fillers in an elastomer matrix. Furthermore, existing intrinsically stretchable interconnects have extremely low optical transmittance (T), so they are not suitable for use as stretchable TCEs for ISOLEDs. To permit escape of photons that are generated in the light-emitting layer through transparent electrodes and substrates, T >85% at 550 nm is normally required.[16,17]

Energy-level alignment at the stretchable TCE/organic interface is also a requirement in the development of highly bright ISOLEDs. TCEs with high work function (WF) >5 eV are preferred for hole injection, whereas low WF <4 eV is necessary for electron injection.[18] To meet these requirements, modified conductive polymers with nanofibril structures, 1D metal nanowires (NWs), 2D MXenes, and graphene can be utilized as alternatives that have high stretchability, high electrical conductivity σ, high T, and tunable WF (Figure 2A).

Nonetheless, due to the inherent trade-off relationships between stretchability and σ, and between σ and T, the design of intrinsically stretchable low-dimensional conductors that meet all these requirements poses a significant challenge. The incorporation of conductive fillers into elastomers increases stretchability (Figure 2B) but decreases T and σ due to the need for a large quantity of conductive fillers to form percolation networks. Consequently, the use of composite methods is more suitable for stretchable interconnect applications.

In contrast, to increase T in TCEs, options such as coating or surface embedding with a small amount of conductive materials on top of elastomers are available (Figures 2C and 2D), but this approach reduces the connectivity of percolation networks compared to composites and therefore sacrifices stretchability. Thus, a rational design of stretchable low-dimensional conductors is essential for both interconnects and TCEs.

From this perspective, we review the noteworthy developments in the use of intrinsically stretchable low-dimensional conductors for display applications, along with our perspective on the advancements of ISOLEDs. Additionally, we propose potential research directions for ISOLEDs that may attract the interest of researchers in this field.

INTRINSICALLY STRETCHABLE INTERCONNECTS

Wearable and stretchable displays require intrinsically stretchable interconnects that maintain the electrical connectivity

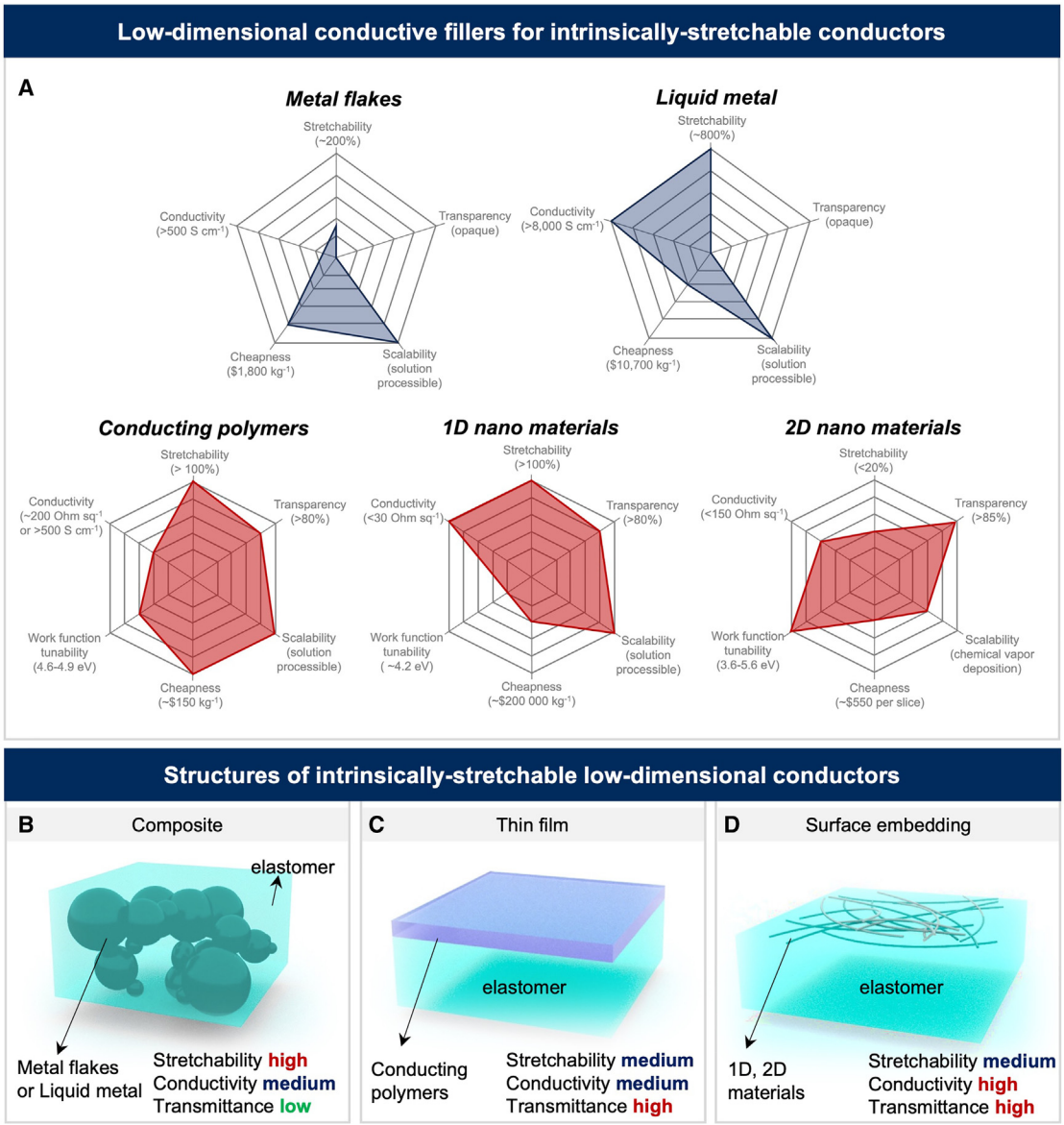

Figure 2. Comparison of intrinsically stretchable conductors that use various of materials and fabrication methods

(A) Comparison of different stretchable interconnects and transparent conductive electrodes using metal flakes, liquid metals, conducting polymers, and 1D and 2D nanomaterials. The axis scale presented in the figure is intended for comparative purposes only and does not represent absolute values.

(B–D) Comparative evaluation of intrinsically stretchable conductors fabricated using (B) composite, (C) thin-film, and (D) surface-embedding methods.

between different components of a device or system even under tensile strain $\varepsilon = 100 \cdot \Delta L/L = 100\%$, where L is length. Persistently pushing the upper limits of maximum tensile strain facilitates the improvement of mechanical reliability at smaller amounts of strain. Therefore, to ensure practical applicability, the stretchability of the interconnects should be maintained well beyond 100%. To achieve this characteristic, composites that consists of elastomers and highly conductive low-dimensional conductors such as metal flakes or liquid-metal particles are widely used.[19]

Incorporation of low-dimensional conductors within the elastomer matrix enables formation of percolation networks, which ensure high σ even under mechanical deformation. For a material to be usable for stretchable interconnects, long-range percolation networks that form within the elastomer matrix must have high σ and negligible resistance change R/R_0 (where R is resistance after stretching and R_0 is the initial resistance) during cycles of stretching and releasing. Additionally, the inherent adhesive properties of the elastomer matrix increase the adhesion between the stretchable interconnects and the substrate.[20] This adhesion is crucial for maintaining the structural integrity of stretchable interconnects. Furthermore, the viscoelastic nature of the stretchable matrix assists in efficient stress relaxation and thereby increases the structural stability of the conductive networks.[21]

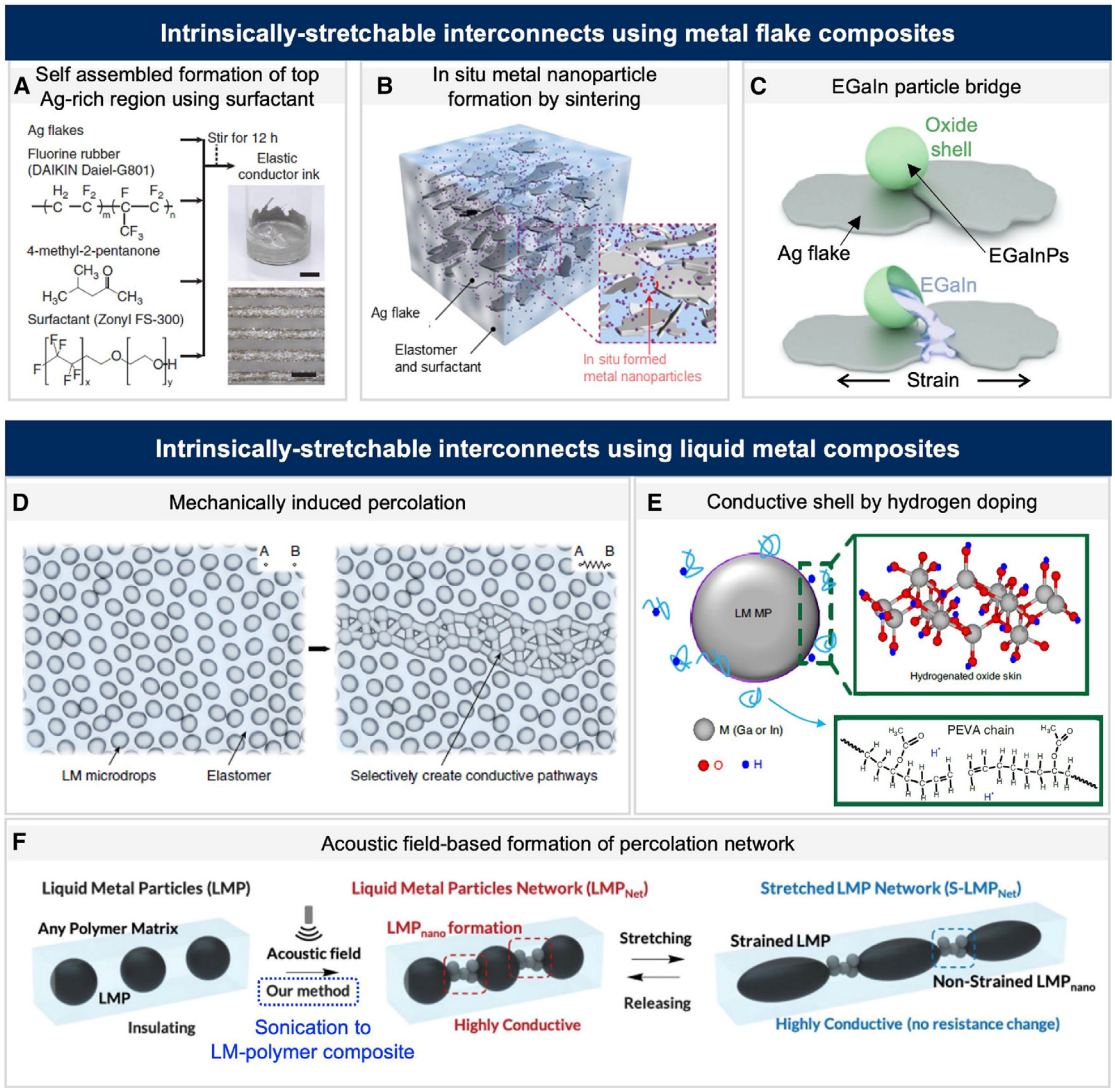

Figure 3. Intrinsically stretchable interconnects that use metal flakes and liquid metal

(A) Formation of a top Ag-rich region due to phase separation between Ag flakes and fluorene surfactant molecules to increase electrical conductivity σ. Scale bar: 100 nm. Reproduced with permission.[25] Copyright 2015, Springer Nature.

(B) *In situ* formation of AgNP bridge achieves high σ even under deformation. Reproduced with permission.[26] Copyright 2017, Springer Nature.

(C) EGaIn particle bridge improves stability in cyclic deformation. Reproduced with permission.[27] Copyright 2018, WILEY-VCH.

(D) Mechanical sintering induces liquid metal rupture to form percolation networks. Reproduced with permission.[28] Copyright 2018, Springer Nature.

(E) Hydrogen doping of oxide shells increases both σ and stability of liquid-metal particles. Reproduced with permission.[29] Copyright 2021, Springer Nature.

(F) Highly conductive percolation networks of liquid-metal particles generated by acoustic field. Reproduced with permission.[2] Copyright 2022, American Association for the Advancement of Science.

Metal-flake low-dimensional conductors are compatible with conventional printing methods and are therefore promising candidates for use as conductive fillers in intrinsically stretchable interconnects.[22] 2D metal flakes have large contact area, which enables them to form conductive percolation networks more effectively than 0D conductive fillers, so use of 2D flakes is a promising approach to developing intrinsically stretchable interconnects that can have both high σ and stretchability.[23] The transport of the electrons through the metal-flake percolation networks occurs by electron tunneling between flakes, so σ is significantly influenced by the distance between them.[24]

By incorporating fluorine surfactants into conductive Ag flakes, the resulting composite experiences a simultaneous increase in the σ and stretchability. This is accomplished by creating Ag-rich regions while simultaneously plasticizing of the elastomer (Figure 3A).[25] The surfactant promotes the aggregation of hydrophobic Ag flakes on the surface of the composite, leading to the formation of a highly conductive percolation network near this surface. As a result, the insulating surfactant

increases the maximum stretchability from 32% to 194% while retaining σ ~500 S cm^{-1}. Blending the conductive ink with fluorine surfactant can reduce the physical distance between metal flakes, but flake particles on the surface of the composite are rigid, so a trade-off can occur between stretchability and σ.

As an alternative, formation of 0D silver nanoparticles (AgNPs) as bridges between Ag flakes in the composite has achieved a high σ of 6,168 S cm^{-1} and a high stretchability of 400%.[26] The Ag metal-flake composite is thermally treated to trigger *in situ* formation of AgNP bridges between Ag flakes (Figure 3B). During this process, the Ag^+ ions diffuse into the elastomer matrix from an Ag_2O layer on the surface of Ag flakes, and the fluorine surfactant molecules can reduce the Ag^+ ions to form AgNPs, which become dispersed between Ag flakes. Therefore, AgNPs serve as both conductive bridges and nanofillers and result in increased mechanical durability. The formation of AgNP bridges effectively reduces the percolation threshold and thereby results in a decrease from 0.111 to 0.046 in the minimum volume fraction of conductive fillers required for the formation of continuous percolation. This decrease indicates an improved connectivity of the conductive network within the composite. The composite demonstrated improved mechanical durability, enduring 95 cycles at 50% strain after the initial five cycles. Although long-term operation endurance remains a concern, these strategies have successfully achieved substantial increases in both σ and mechanical stretchability of intrinsically stretchable interconnects.

Use of hybrid materials that combine the strengths of different conductive materials is also a promising strategy to create resilient and durable interconnects. The incorporation of eutectic gallium-indium (EGaIn) particles with Ag flakes results in a composite that has a superior σ of 8,331 S cm^{-1} and an R/R_0 of ~8 after 10,000 cycles of stretching to ε = 800% and then releasing.[27] This extraordinary mechanical stability occurs because EGaIn particles form conductive anchors between Ag flakes (Figure 3C). EGaIn particles can maintain their particle structures in the composite by forming insulating oxide shells. Under mechanical deformation, oxide shells open and release EGaIn; this process results in formation of conductive bridges between Ag flakes.

Due to superior mechanical stability and high σ of EGaIn, it has also been used as a promising conductive filler without hybridizing with other low-dimensional materials. By dispersing EGaIn in elastomeric polymers, it can be stabilized in the form of particles.[30] However, the low-dimensional spherical shape of the percolation units and the low σ caused by the oxide shells pose significant challenges for intrinsically stretchable conductors that use liquid metals.

Mechanical force (i.e., mechanical sintering) applied to the EGaIn composite can rupture EGaIn particles and lead to the formation of a conductive path that has significantly increased σ (Figure 3D).[28] The percolation induced by mechanical sintering occurs because the oxide shells break, the particle ruptures, and then a new oxide shell forms to restabilize the structure. The liquid-metal composite had an initial σ of 1,370 S cm^{-1} after mechanical sintering and a negligible R/R_0 of ~0.97 after 10^6 cycles of stretching to ε = 40%.

Hydrogen doping of oxide shells can achieve exceptional σ and stretchability without causing any structural alterations (Figure 3E).[29] Ultrasonication of a mixture of bulk EGaIn, PEVA, and a free-radical initiator (dicumyl peroxide) forms liquid-metal particles and generates primary radicals. Primary radicals initiate electron transfer, which triggers the generation of hydrogen radicals, which play a crucial role in the formation of metal–O^{2-}–H^+ on the surface of the liquid-metal particles. The H-doping of the oxide shell induces n-type conductivity by elevating the Fermi energy to above the conduction band minimum and greatly increases σ from 1 to 25,000 S cm^{-1}. Moreover, the adsorption of polymer on the surface of EGaIn particles after H-doping allows the doped particles retain their structure under strain, in contrast to the undoped particles that experience rupture of particle structure under strain. The stretchable interconnect using H-doped EGaIn particles showed an excellent mechanical durability of R/R_0 = 0.8 after 1,000 cycles of stretching at ε = 500%.

Acoustic fields can also induce formation of EGaIn NPs, and this phenomenon represents another promising approach to fabricate highly conductive and highly stretchable liquid-metal composites.[2] The composite exhibits σ >10^4 S cm^{-1} and R/R_0 ~10 under ε = 4,000% and R/R_0 ~1.25 after 1,200 cycles of stretching at ε = 500%. The fabrication process involves exposing the liquid-metal composite to an acoustic field in a water bath, enabling the formation of percolation networks comprising large EGaIn particles (~2 μm) interconnected by EGaIn NPs (Figure 3F). The percolation network, interconnected by EGaIn NPs, effectively prevents the rupture of large particles during deformation by creating additional pathways for strain dissipation through NP bridges. This remarkable phenomenon significantly enhances the toughness of the liquid-metal composite.

Structurally stable percolation networks composed of metal flakes, liquid metals, or both have enabled significant increases in σ and mechanical durability of intrinsically stretchable interconnects (Table 1). Despite the significant progress made in σ and stretchability, the interface between stretchable interconnects and other conductive materials continues to pose a significant obstacle due to the lack of satisfactory mechanical and chemical stability. When in contact with metals, the corrosive nature of liquid metals at the liquid-metal/metal interface requires careful consideration of material compatibility between liquid metals and the other metals involved. The current state of the interface falls short of meeting the required standards, demanding further improvements to ensure reliable performance and durability. Moreover, although tailoring the adhesion properties of the elastomer matrix can increase the overall adhesion between the liquid-metal composite film and the substrate, the high surface tension of liquid metals still presents a challenge in achieving strong adhesion at the interface with other stretchable conducting materials. Poor adhesion can decrease charge-injection efficiency at the interface, particularly during stretching.

Patterning of intrinsically stretchable interconnects also poses a significant challenge against their high-resolution array applications. Recent research has made progress in fabricating micrometer-scale (25 μm) patterns of conductors by using a composite of liquid metal and rigid photoresist.[2] However, achieving stretchable nanopatterned liquid-metal composites remains difficult because the task requires simultaneous

Table 1. Comparison of intrinsically stretchable interconnects

Category	Composition	σ (S cm^{-1})	Static stretching		Cyclic stretching		
			R/R_0	Maximum ε (%)	R/R_0	ε (%)	Cycles
Metal flake	fluorine rubber/fluorine surfactant/Ag flakes[25]	738	0.25	215	>10	10	1,000
	fluorine rubber/fluorine surfactant/Ag flakes[26]	6,168	0.24	400	~100	50	100
	PAAm-alginate hydrogel/Ag flakes[31]	350	~70	250	~3	100	1,000
	PDMS-MPU$_{0.4}$-IU$_{0.6}$/Ag flakes[32]	9,990	~5	120	~1.15	30	1,000
	viscoelastic polymer (PTA, PEG, aniline) Ag flakes[33]	~10,000	~10	1,000	~3	1,000	1,000
Metal-flake/liquid-metal hybrid	EVA/Ag flakes/EGaIn[27]	8,331	6.3	900	~8	800	10,000
	PVA-borax hydrogel/Ag flakes/EGaIn[34]	700	~10	100	~7	50	405
Liquid metal	PDMS/EGaIn[28]	1,370	~1.1	50	~0.97	40	1,000,000
	PEVA/DCP/EGaIn[29]	25,000	~0.71	100	0.8	500	1,000
	elastomers/EGaIn[2]	21,000	~10	4,000	~1.25	500	1,200
	pp-TPU/EGaIn[35]	22,532	30	2,266	~1.6	100	10,000

improvements in resolution, stretchability, and even higher σ to minimize voltage drop. Current stretchable interconnects that use metal flakes and/or liquid metals have $\sigma \sim 10^4$ S cm^{-1}, which is still more than an order of magnitude lower than that of bulk metal electrodes (>10^5 S cm^{-1}). To overcome this limitation, efforts should be directed toward achieving a uniform distribution of liquid-metal NPs and to increase the σ of percolation networks within the elastomer matrix; achieving these goals will help to reduce processing variation and to maintain consistent σ throughout the patterned electrodes.

INTRINSICALLY STRETCHABLE TCEs THAT USE CONDUCTING POLYMERS

Numerous conducting polymers are available; examples include poly(3,4-ethylenedioxythiophene):poly(styrenesulfonate) (PEDOT:PSS), polyacetylene (PA), polyaniline (PANI), polypyrrole (PPy), polythiophene (PTH), and polyfuran (PF). Extensive studies have been conducted on synthesizing these conducting polymers, analyzing their conduction mechanisms, and developing post-treatment methods to increase their σ.[36–39]

Among the various conducting polymers, PEDOT:PSS has distinctive advantages. It can be easily fabricated with high mechanical compliance. Additionally, PEDOT:PSS can possess high σ, high optical *T*, and an adjustable *WF*. Its commercial viability has also demonstrated by a wide range of commercialized products. As a result, PEDOT:PSS stands out as an intrinsically stretchable conducting polymer for wearable applications.

PEDOT:PSS consists of conducting/hydrophobic positively charged PEDOT and insulating/hydrophilic negatively charged PSS.[40] The high σ of PEDOT:PSS is attributed to its primarily doped and conjugated PEDOT backbone, whereas the tunable stretchability and *WF* originate from the presence of the soft PSS domain that has high ionization energy.[41] An increase in stretchability is often accompanied by degradation of other electrical and optical properties, and this trade-off complicates the task of simultaneously achieving all requirements for TCEs in ISOLEDs. Therefore, to fully utilize the potential of PEDOT:PSS, a secondary doping process is essential.

Secondary dopants can permanently alter the morphology of the PEDOT:PSS and thereby yield improved stretchability and σ of the film. The σ of PEDOT:PSS is mainly governed by intragrain and intergrain charge transport.[42] Numerous methods have been implemented to decrease π-π stacking and interlamellar distances within a PEDOT domain and to simultaneously elongate conductive pathways between adjacent PEDOT grains (Table 2).[42,58] The addition of polar solvent and surfactants can hinder the Coulombic interaction between PEDOT and PSS, and thereby cause close packing of conjugated PEDOT backbones. This change facilitates the transport of charge carriers along PEDOT chains, so σ increases. This phenomenon is referred to as the screening effect.

Post-treatment with strong acid has increased σ of PEDOT:PSS electrode by three orders of magnitude from 1 S cm^{-1} to >4380 S cm^{-1} (Figure 4A).[43] This increase was achieved by dipping as-cast PEDOT:PSS film into strong acid such as H_2SO_4. The concentrated H_2SO_4 undergoes autoprotolysis forming $H_3SO_4^+$ and HSO_4^-, acting as counterions for the negatively charged PSS and positively charged PEDOT chains, respectively. These counterions effectively reduce the Coulombic interaction and stabilize the segregated states of positively charged PEDOT and negatively charged PSS chains. The strong screening effect causes significant structural rearrangement in the granular morphology of PEDOT:PSS to form a crystalline nanofibrillar structure; the H_2SO_4 post-treatment also removes residual PSS chains, resulting in a significant increase in σ.

Furthermore, employing a strong acid post-treatment on a blend of poly(ethylene glycol)-block-poly(propylene glycol)-block-poly(ethylene glycol) (PEO_{20}-PPO_{70}-PEO_{20} [P123]) has enabled fabrication of highly conductive, stretchable, and transparent PEDOT:PSS electrodes (Figure 4B).[46] PEDOT:PSS solution mixed with P123 was spin coated on the substrate and then soaked in concentrated H_2SO_4. The hydroxyl group of PEO forms hydrogen bonds with PSS, so the addition of P123 can separate PEDOT and PSS chains. Subsequently, P123 molecules can undergo condensation polymerization under H_2SO_4. The crosslinked P123 causes aggregation of a large PEDOT

Table 2. Comparison of intrinsically stretchable TCEs

Category	Composition	σ/R_s (S cm^{-1}/Ohm sq^{-1})	T (%)	WF (eV)	Static stretching		Cyclic stretching		
					R/R_0	ε (%)	R/R_0	ε (%)	Cycles
Conducting polymer	concentrated H_2SO_4[43]	>4,000/–	90	–	–	–	–	–	–
	ethylene glycol + CH_4SO_3[44]	3,560/–	92	–	–	–	–	–	–
	shearing method[45]	4,600/–	97	–	–	–	–	–	–
	DMSO + Zonyl[40]	120/–	93	–	–	–	–	–	–
	PEO-PPO-PEO+H_2SO_4[46]	1,700/–	89	–	1.04	40	1.25	40	1,000
	STEC[47]	3,100–4,100/–	96	–	<1	100	~1	100	1,000
	EMIM:TCB ionic liquid[48]	1,200/–	–	–	~2	40	–	–	–
	ION E Zwitter ion PSSNa[41]	>1,000/–	–	5.35/4.73	–	–	–	–	–
	PR-PEGDA[49]	3,000–6,000/–	–	–	2.5	100	2	100	500
1D	SWNT[50]	–/500	87	–	1.45	40	1.14	40	14
	AgNW[51]	–/15	83	–	10	40	4.3	30	1,500
	AgNW:GO[52]	–/14	82.5	–	3.2	40	3	40	100
	AgNW:PEI:ZnO[53]	–/40	85	–	5	40	11	40	500
2D	graphene[54]	–/30	~90	5.95	–	–	–	–	–
	MXene[55]	–/115	85	5.1	–	–	–	–	–
	MXene/PFI[56]	–/97.4	90	5.84	–	–	–	–	–
	graphene/AgNW hybrid[57]	–/22	88	5.69/3.63	3.9	40	6.1	40	500

core and yields an increased σ of 1,700 S cm^{-1} and stretchability of >40%.

Use of ionic additives can also simultaneously achieve high σ and stretchability (Figure 4C).[47,48] Water-soluble ionic liquids that contain highly acidic anions can induce secondary doping and a charge-screening effect, which together cause a morphological transition from granular structure to crystalline and interconnected PEDOT nanofibrillar structures. Concurrently, the small ionic species tend to reside in regions that are relatively disordered, and this distribution further softens the PEDOT:PSS matrix. As a result, incorporation of ionic liquids into PEDOT:PSS yields a high σ of 4,100 S cm^{-1} and an ability to endure ε >100%.[47]

PEDOT:PSS has a high WF >4.9 eV that is favorable for efficient hole injection in ISOLEDs. To use PEDOT:PSS as the cathode, the WF must be as low as possible to increase the electron-injection ability. To achieve low WF, the interface must be modified using non-conjugated polyelectrolytes that bear abundant amine groups; examples include poly(ethyleneimine) (PEI) and polyethyleneimine ethoxylated (PEIE).[60–63] However, spin coating of these materials on top of PEDOT:PSS electrode inevitably reduces its stretchability due to the use of polar solvents such as isopropyl alcohol (IPA) or 2-methoxyethanol, which can wash out the soft PSS groups and secondary dopants during the spin-coating process.[41] This reduction in stretchability can be overcome by using 4-(3-ethyl-1-imidazolio)-1-butanesulfonate (ION E) and sodium polystyrene sulfonate (PSSNa) with high molecular weight (Figure 4D).[41] ION E has low solubility in the polar solvents, so loss of ionic species during the interfacial modification process can be reduced. Moreover, long PSS chains further increase the crack-onset strain by suppressing formation of microcracks. Consequently, the use of ION E and PSSNa enabled the PEDOT:PSS electrode to fulfill all the essential requirements including σ >1,000 S cm^{-1}, stretchability >70%, and a lowered WF of 4.6 eV.

The formation of a mechanically interlocked network within the PEDOT:PSS film by using a polyrotaxane (PR) crosslinker also increases the film's σ and stretchability. PR is composed of a polyethylene glycol (PEG) backbone and sliding cyclodextrins with PEG methacrylate side chains (Figure 4E).[49] The sliding cyclodextrins units prevent PEG crystallization, which increases the stretchability of the PEDOT:PSS. Subsequent H_2SO_4 treatment increases the σ of PEDOT:PSS/PR to >2,700 S cm^{-1}, and it can be further improved to 6,000 S cm^{-1} at ε = 100% because the strain increases alignment of the chains.

To use PEDOT:PSS/PR as a stretchable TCE for ISOLEDs, energy-level alignment at the stretchable electrode/organic material interface is important to attain a highly efficient organic light-emitting diodes. To lower the WF of the PEDOT:PSS/PR electrode, the surface has been modified using a blend of poly(9,9-bis(3'-(N,N-dimethyl)-N-ethylammonium-propyl-2,7-fluorene)-alt-2,7-(9,9-dioctylfluorene)) dibromide (PFN-Br) and PEIE (Figure 4F).[59] The PEDOT:PSS/PR electrode modification enables the ISOLED to turn on at 5 V and reach a maximum brightness of 7,450 cd m^{-2} at 15 V, with a corresponding maximum current efficiency (CE) of ~5.3 cd A^{-1}.

Because of the high T, stretchability, and uniformity of the PEDOT:PSS conductive polymer, PEDOT:PSS electrodes can be an appropriate material for cathode and anode in ISOLEDs. Their use overcomes the disadvantage of using metal NWs, which must have numerous internal junctions to maintain high σ. However, the junctions are vulnerable to failure due to inevitable joule heating during device operation. This trait of metal NWs impedes uniform injection and spreading of charges in

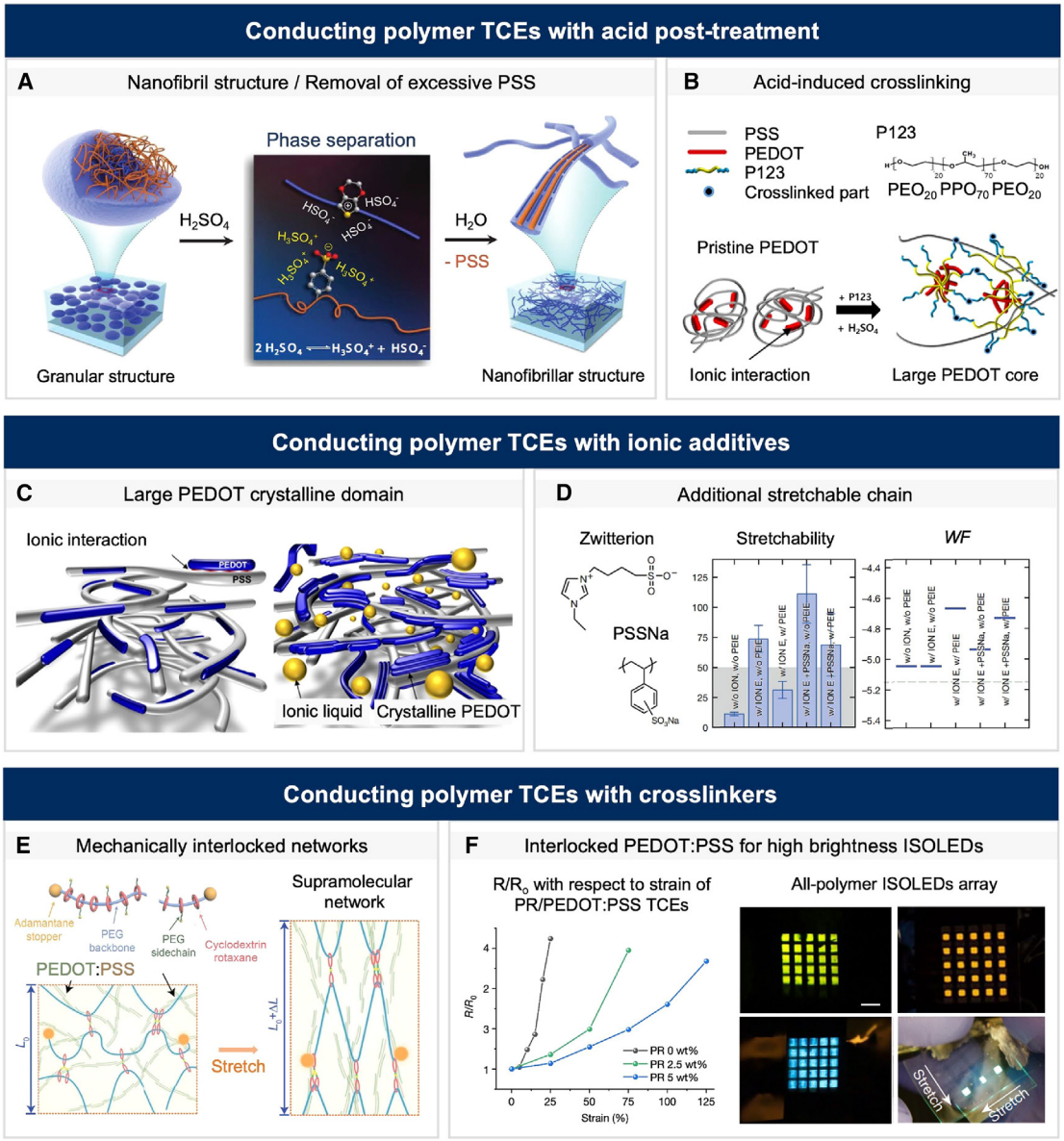

Figure 4. Strategies to improve the σ and stretchability of conductive polymer (PEDOT:PSS) TCEs

(A) Electrical σ increase with structural rearrangement from granular to nanofibrillar structure after acid post-treatment. Reproduced with permission.[43] Copyright 2014, WILEY-VCH.

(B) Increase in σ and stretchability due to the phase separation of PEDOT:PSS and acid-induced crosslinking of P123 chains. Reproduced with permission.[46] Copyright 2018, American Chemical Society.

(C) Simultaneous attainment of high σ and stretchability after the addition of ionic liquids, which provides a strong electrostatic screening effect and enables the close packing of crystalline PEDOT domains. Reproduced with permission.[47] Copyright 2017, American Association for the Advancement of Science.

(D) *WF* modulation with maintained high σ and stretchability using Zwitterion (ION E). Long PSS chains that remain after wash off during the interfacial modification with PEIE can further increase the stretchability of PEDOT:PSS TCEs. Reproduced with permission.[41] Copyright 2021, Springer Nature.

(E) Enhancement of conductivity and stretchability with the formation of mechanically interlocked networks by crosslinking of polyrotaxane crosslinker bearing sliding cyclodextrin units. Reproduced with permission.[49] Copyright 2022, American Association for the Advancement of Science.

(F) ISOLEDs with high maximum brightness and current efficiency using intrinsically stretchable polyrotaxane/PEDOT:PSS TCEs. Photographs represent all-polymer ISOLED arrays with different colors while being stretched. Scale bar: 2.5 mm. Reproduced with permission.[59] Copyright 2022, Springer Nature.

the light-emitting layer (EML). In contrast, PEDOT:PSS does not undergo joule heating and therefore endows ISOLEDs with high luminance.[59] Nevertheless, PEDOT:PSS still has a lower σ than other TCE materials such as metal NWs, graphene, and MXene. Therefore, the σ of PEDOT:PSS electrodes must be further increased.

INTRINSICALLY STRETCHABLE TCEs THAT USE LOW-DIMENSIONAL CONDUCTORS

Intrinsically stretchable low-dimensional conductors are being developed as replacements for conventional TCEs such as indium tin oxide that are inherently brittle and therefore unsuitable for use in wearable and stretchable light-emitting devices.[12–14] PEDOT:PSS is a conducting polymer that has a high *WF* that facilitates hole injection and is a promising candidate for use as a stretchable anode. However, surface modifications using such as PEI or PEIE to lower the *WF* of PEDOT:PSS will dedope the $PEDOT^+$ and thereby significantly reduce its σ.[64] Therefore, low-dimensional conductors that exploit silver NWs (AgNWs), carbon nanotubes (CNTs), graphene, or MXenes have been incorporated into elastomers for stretchable applications as alternatives (Table 2). These materials are either transferred to or deposited on the surface of the elastomer matrix to achieve high T and σ simultaneously.[11]

Single-walled CNTs (SWNTs) were used as an intrinsically stretchable anode and cathode for the first time in 2011.[50] SWNT networks were embedded using poly(tert-bultylacrylate) (PtBA), which is a shape-memory polymer that has a low glass transition temperature (T_g) of 56°C. The resulting SWNT stretchable electrode had sheet resistance (R_s) = 500 Ω sq^{-1} and T = 87% at 550 nm. The stretchable EML, composed of a light-emitting polymer, an electrolyte, and a salt, was sandwiched between two SWNT stretchable TCEs. However, the SWNT stretchable electrode has high R_s, so the maximum luminance (L_{max}) reaches only 200 cd m^{-2} with V_{on} = 4.5 V.

To increase the σ of stretchable TCEs, CNTs have been replaced with AgNWs as the conductive filler due to their high σ and T, but their high surface roughness can lead to significant leakage current during device operation.[65] To solve this problem, AgNWs are inlaid in the elastomer with part of their surface exposed to air (Figure 5A).[66] The interaction between the elastomer matrix and AgNWs strongly influences the stretchability of the TCEs. Soft elastomer matrices such as polyurethane acrylate (PUA) can uniformly distribute stress by limiting NW sliding and the consequent distortion of AgNW junctions[14]; this process yielded stretchable TCEs with R_s = 15 Ω sq^{-1} and T = 83% that can withstand >100 peel-off tests using Scotch tape.[51] ISOLEDs that use AgNWs in PUA stretchable electrodes as both anode and cathode had L_{max} = 2,200 cd m^{-2} (at 21 V), maximum ε = 120%, and maximum *CE* = 11.4 cd A^{-1}.

The mechanical durability of stretchable TCEs is a significant determinant of the maximum tensile strain that the ISOLED can withstand. Sliding and distorting of AgNWs under tensile strain are unfavorable, so one possible approach to avoid these problems is to strengthen junctions in AgNW percolation networks. Various physical and chemical methods have been used to weld the junction and increase the σ and stretchability of AgNWs.[65] However, some methods can result in strong binding between AgNWs and the substrate and are therefore not suitable for stretchable applications because these bonds hinder transfer of AgNWs from the substrate to the elastomer.

This problem can be solved by using graphene oxide with abundant oxygen-containing moieties to adhere to AgNWs and solder the junction by exploiting the capillary effect during solvent evaporation (Figure 5B).[52] The resulting welded AgNW percolation networks have been successfully transferred to the elastomer matrix and yielded R_s = 14 Ω sq^{-1}, T = 88%, and a maximum ε = 130%.

The efficiency of ISOLEDs is directly determined by the electronic energy-level alignment at the stretchable TCE/organic material interface. Achieving an anode that has high *WF* comparable to that of indium tin oxide (ITO; ~4.7 eV) and a cathode that has low *WF* compared to the LiF/Al electrode (~4 eV) is very difficult task when the same intrinsically stretchable material is used as both anode and cathode. The charge-injection capability of a stretchable TCE is mainly affected by two factors: the electrical contact area with the adjacent organic materials and the *WF*. In most stretchable TCEs that use AgNWs embedded in the elastomer, the electrical contact area is small, which hinders the charge injection from the stretchable TCEs to the organic material. Furthermore, AgNWs with a *WF* of 4.25 eV are not sufficient for efficient injection of holes or electrons.[69]

To increase the contact area, AgNW networks can be directly coated on a stretchable EML by using successive ZnO- and PEIE-coating steps to yield AgNW networks embedded in a composite of ZnO and PEIE.[53] This structure increases the electron injection capability by increasing the electrical contact area of AgNWs (Figure 5C). However, direct solution coating on the stretchable EML may reduce the reliability of the ISOLED. Increasing the processing temperature to >150°C after the solution process effectively removes the residual solvent and increases the reproducibility.[70] However, most intrinsically stretchable materials have a low T_g, so they are damaged by this high-temperature processing, and this trait impedes use of this method to attain efficient and reliable ISOLEDs.

The charge-injection capability of stretchable TCEs can be improved by using 2D conducting materials (Figure 5D).[67] For instance, a *WF*-tunable polymer conducting polymer deposited on top of a graphene electrode can yield a *WF* gradient in the thickness direction, with surface *WF* = 5.95 eV.[54] The OLEDs fabricated on the surface-modified graphene electrode attained maximum *CE* = 98.1 cd A^{-1}; this result indicates that graphene is a promising electrode material for optoelectronic applications. Furthermore, graphene scrolls placed between stacked graphene layers can bridge cracks and maintain conduction paths during stretching (Figure 5E).[68]

Many research efforts primarily concentrate on stretchable anodes without addressing the need to tune the charge injection properties of stretchable cathodes (Table 2). Drawing on the aforementioned insights, an effective approach is to form a 2D-contact stretchable electrode by introducing graphene with graphene scrolls on top of a stretchable electrode that uses AgNW (Figure 5F).[18,71] The graphene layer modified the *WF*, spread the charges, prevented inward diffusion of oxygen and moisture, and increased the electrical contact area without sacrificing mechanical stretchability. Surface modification then adjusted the *WF*s of the stretchable TCEs: perfluorosulfonic acid yielded the highest *WF* (5.69 eV), whereas anionic crown-conjugated polyelectrolyte yielded the lowest *WF* (3.57 eV). Fine-tuning the charge-injection properties of the stretchable anode and cathode yielded the highest ISOLED *CE* (20.3 cd A^{-1}). These

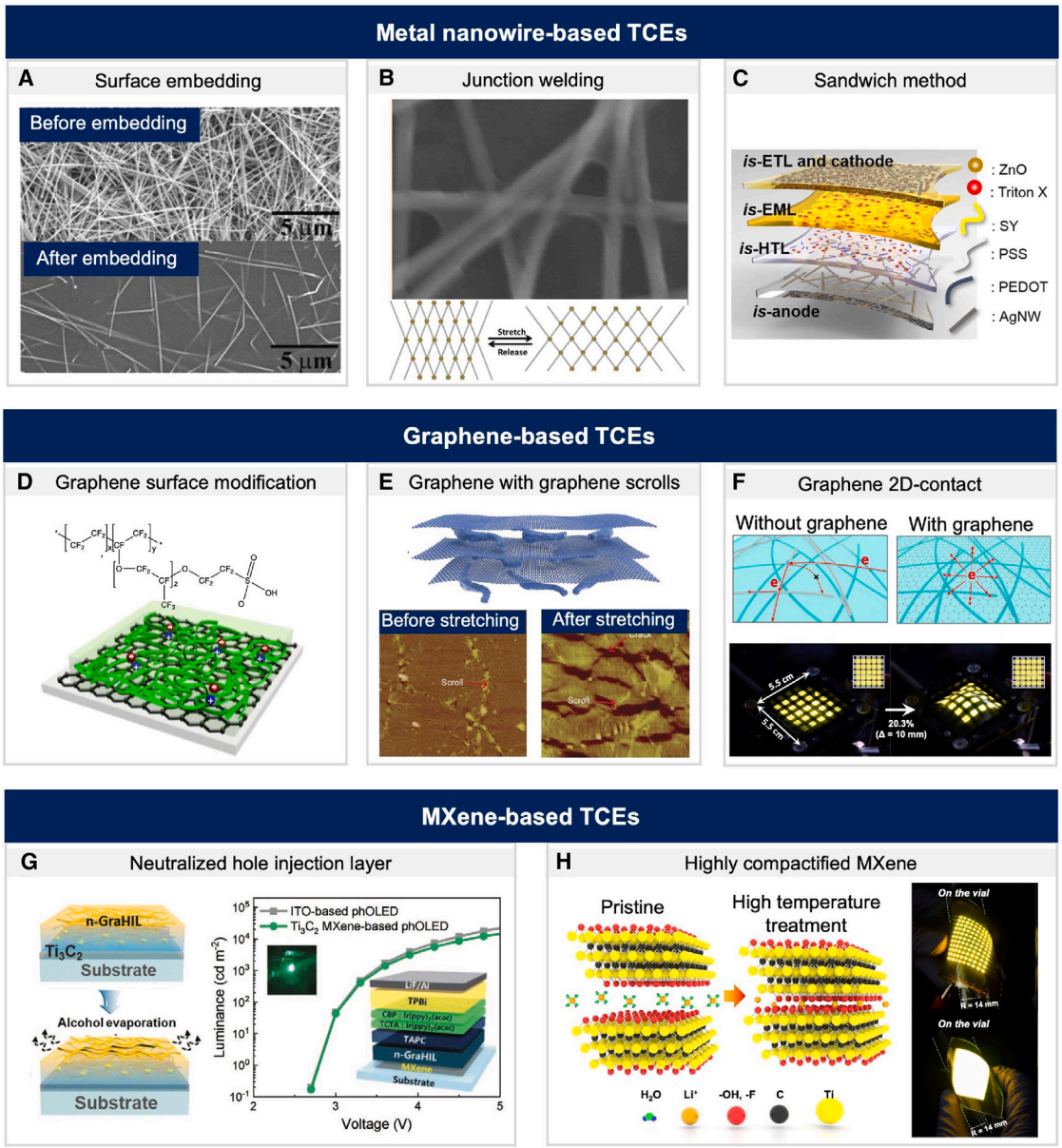

Figure 5. Intrinsically stretchable TCEs that use low-dimensional material

(A) Metal nanowires embedded in the elastomer matrix to increase stretchability. Reproduced with permission.[66] Copyright 2012, WILEY-VCH.

(B) Top: scanning electron microscopy (SEM) image of welded junctions. Bottom: schematic illustration of stretching mechanism of AgNW percolation networks after welding process. Reproduced with permission.[52] Copyright 2014, American Chemical Society.

(C) Metal nanowires sandwiched between a film of ZnO and a film of PEIE composite to improve the electron-injection capabilities. Reproduced with permission.[53] Copyright 2021, American Association for the Advancement of Science.

(D) Graphene with surface modification. Reproduced with permission.[67] Copyright 2018, Springer Nature.

(E) Graphene with graphene scrolls enables a stretchable electrode. Top: schematic of graphene and graphene scrolls. Bottom: atomic force microscopy (AFM) images of graphene and graphene scrolls before and after stretching. Reproduced with permission.[68] Copyright 2017, American Association for the Advancement of Science.

(F) 2D contact stretchable electrode (TCSE) that introduces graphene on top of surface-embedded AgNW percolation networks. Top: schematic of TCSEs. Bottom: a 3 inch large-area passive-matrix ISOLED using TCSEs. Reproduced with permission.[57] Copyright 2022, WILEY-VCH.

(G) Left: MXene with chemically neutralized hole-injection layer. Right: luminance-voltage curve of OLEDs using MXene and ITO, respectively. Reproduced with permission.[55] Copyright 2020, WILEY-VCH.

(H) Left: schematic image of reduced *d*-spacing of MXene after treatments. Right: large-area passive-matrix OLED using MXene as the electrode. Reproduced with permission.[56] Copyright 2022, WILEY-VCH.

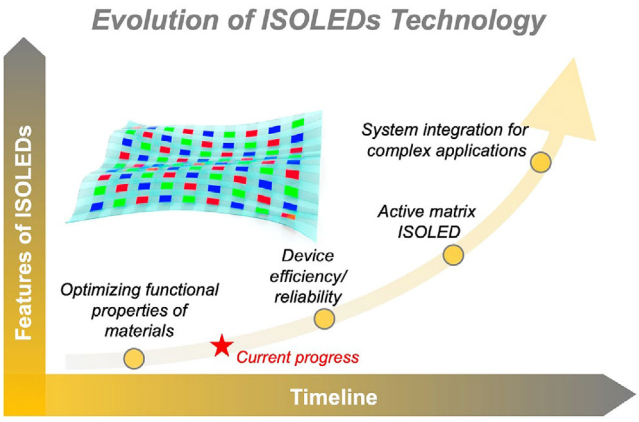

Figure 6. Evolution of ISOLED technology

electrodes were successfully applied to 3 inch 5 × 5 passive-matrix ISOLEDs.

MXene is a 2D interlayer that can be used to replace graphene. MXenes constitute a family of 2D materials that have metallic σ and high *T*. The most common is titanium carbide ($Ti_3C_2T_x$), which has abundant surface groups that contain F and O.[72] However, MXene degrades easily, especially in the presence of moisture, and this instability limits their application in solution-processed optoelectronic devices. This process entails an exfoliation step, during which Li^+ are intercalated and can be easily hydrated when exposed to air; this process enlarges the *d*-spacing and decreases the σ.[56] To solve this problem, chemical neutralization of conducting polymer PEDOT:PSS provides a solution to the chemical instability of MXene (Figure 5G).[55] OLEDs that use the modified PEDOT:PSS and MXene electrodes have comparable *CE* to that of ITO-based devices; this result proves that overcoming the instability of MXene could facilitate its application in optoelectronics.

To increase the environmental stability of MXene, the diffusion of moisture into the interlayer spacing must be minimized.[56] The interlayer spacing can be derived from the *d*-spacing that is determined by Bragg's law, which is

$$2d \times \sin\theta = n\lambda,$$

where *d* is the spacing between planes of atoms that induce diffraction peaks, θ is the X-ray diffraction incident beam angle, *n* is a positive integer, and λ is the wavelength of the incident beam. The interlayer spacing can be obtained by subtracting the thickness (≈1 nm) of the $Ti_3C_2T_x$ MXene layer from *d*. The 2D layered structure of MXene allows moisture to diffuse both vertically and laterally. High-temperature annealing of MXene reduces the *d*-spacing of MXene from 0.33 to 0.06 nm and thereby effectively blocks lateral moisture diffusion. Additionally, deposition of a PFSA barrier layer onto MXene (*WF* = 5.84 eV, R_s = 97.4 Ω sq^{-1}) impedes perpendicular moisture diffusion between MXene flakes. Consequently, MXene that has been treated in this way undergoes a negligible change in R_s and *WF* after exposure to air for >22 days. The MXene TCE has also been used in a large-area 10 × 10 passive-matrix OLED (Figure 5H). Therefore, an environmentally stable MXene electrode is a potential candidate as a 2D contact layer for stretchable TCEs that use AgNWs.

In conclusion, the integration of low-dimensional materials has facilitated the rapid development of highly stretchable, conductive, transparent, and *WF*-tunable TCEs which are promising as both anode and cathode in ISOLEDs. Despite the significant development in stretchable TCEs, the *CE* of ISOLED still lags behind than that of rigid devices. Therefore, future research efforts should attempt to design stretchable charge transport materials, light-emitting materials, and device fabrication protocols to increase the efficiency of ISOLEDs.

OUTLOOK

In comparison to conventional OLEDs fabricated on rigid glass substrates, stretchable displays demonstrate notable deficiencies in efficiency, maximum luminance, and operational stability. This disparity can be ascribed to the lack of established standards, design strategies, and processing techniques that are specific to stretchable materials and devices. The field of ISOLED development remains in its nascent stages (Figure 6). Accelerating the progress of ISOLEDs requires optimization of the functional properties of intrinsically stretchable conducting, semiconducting, and insulating materials.

In this perspective, we have explored recent advances in utilization of intrinsically stretchable low-dimensional conductors for ISOLED applications. The incorporation of metal flakes or liquid metal within a thermal plastic elastomer matrix has yielded stretchability in interconnects. The formation of nanometer-scale particles between micrometer-scale particles or flakes, along with the maintenance of good electrical contact among them, helps to increase both electrical σ and mechanical stretchability. To effectively employ such interconnects as driving circuits for ISOLEDs in the future, the following aspects need to be carefully considered. Firstly, electrochemical stability is important because undesirable reactions can lead to deterioration of the light-emitting properties of ISOLEDs. Secondly, resistance to organic solvents is crucial for the integration of various stretchable materials and devices. A potential solution in the future could involve the implementation of a crosslinked elastomer network. Thirdly, achieving nanometer-scale photopatternability becomes necessary for seamless integration with complex electric circuits. Lastly, ensuring environmental stability of interconnects is crucial to improve the overall reliability of the system.

In the case of intrinsically stretchable TCEs, the primary challenge is to increase stretchability while simultaneously preserving other functional properties. The manipulation of chemical interactions between low-dimensional materials and elastomers will strongly contribute to the mechanical properties of intrinsically stretchable TCEs. Additionally, a suitable match in stretchability between the intrinsically stretchable TCEs and adjacent layers in the ISOLED is essential to prevent detachment at the interface during stretching, which can occur due to contraction perpendicular to the substrate. Furthermore, strengthening interfacial adhesion without decreasing the charge-injection property could increase the stretchability of ISOLEDs.

However, the development of a reliable, stretchable, and transparent encapsulation poses the most significant challenge in the development of ISOLEDs. Achieving stretchability necessitates the entanglement of polymer chains that possess a significant amount of free volume. In contrast, barrier properties demand closely packed molecules. This trade-off relationship between stretchability and barrier properties adds complexity to the process of designing suitable encapsulations that can rival the effectiveness of glass lid encapsulations. Consequently, an innovative approach to designing stretchable encapsulations becomes imperative.

Then, full utilization of ISOLEDs as wearable devices for visualization of complex signals will require development of active-matrix ISOLEDs with pixelization and individual driving circuits, using both intrinsically stretchable TCEs and interconnects in one system. Active-matrix ISOLED arrays encompass complete layers of stretchable cathodes, stretchable charge-transport materials, stretchable light-emitting materials, and stretchable anodes. However, the stretchable anode overlays thin-film transistor (TFT) arrays that act as the active matrix. By utilizing stretchable interconnects as the source, drain, and gate electrodes of the transistors, the stretchability of the array can be increased. Integration of ISOLEDs onto TFT backplanes is possible in theory, but the stacking of multiple layers of conducting, semiconducting, and insulating materials with specific patterns presents an extremely challenging task due to their different solvent miscibility. Precise control of each layer's pattern from the back plane to the ISOLED on top is critical. Lamination is the most widely used method to fabricate ISOLED, but to improve the process yield, the complexity of the process must be reduced.

Finally, integration of ISOLED with other functional devices is considered the ultimate goal for wearable displays. Wearable displays will have a wide range of applications from health monitoring to augmented reality and therefore will collect and process data, in addition to displaying information. Therefore, wearable displays must be integrated with power supplies, wireless signal transmission and receiving units, and signal processing units. The resulting devices will have a broad range of applications.

ACKNOWLEDGMENTS

This work was supported by a National Research Foundation of Korea (NRF) grant funded by the Korean government (Ministry of Science, ICT & Future Planning) (2016R1A3B1908431), LG Display under the LGD-SNU Incubation Program (2021005682), and the Creative Materials Discovery Program through the NRF funded by Ministry of Science and ICT (2018M3D1A1058536). This research was also supported by the Pioneer Research Center Program through the NRF funded by the Ministry of Science, ICT and Future Planning (grant no. 2022M3C1A3081211).

AUTHOR CONTRIBUTIONS

H.Zhou, K.-N.Kim, and M.-J.Sung, co-wrote the initial manuscript. T.-W.Lee. proposed the topic, and H.Zhou, K.-N.Kim, M.-J.Sung., and T.-W.Lee. revised the manuscript. All authors contributed to the discussion and revision of the manuscript. H.Zhou, K.-N.Kim, and M.-J.Sung contributed equally to this work.

DECLARATION OF INTERESTS

The authors declare no competing interests.

REFERENCES

1. Lee, Y., Chung, J.W., Lee, G.H., Kang, H., Kim, J.-Y., Bae, C., Yoo, H., Jeong, S., Cho, H., Kang, S.-G., et al. (2021). Standalone real-time health monitoring patch based on a stretchable organic optoelectronic system. Sci. Adv. *7*, eabg9180.
2. Lee, W., Kim, H., Kang, I., Park, H., Jung, J., Lee, H., Park, H., Park, J.S., Yuk, J.M., Ryu, S., et al. (2022). Universal assembly of liquid metal particles in polymers enables elastic printed circuit board. J. Sci. *378*, 637–641.
3. Xu, J., Wang, S., Wang, G.-J.N., Zhu, C., Luo, S., Jin, L., Gu, X., Chen, S., Feig, V.R., To, J.W.F., et al. (2017). Highly stretchable polymer semiconductor films through the nanoconfinement effect. Science *355*, 59–64.
4. Hu, H., Huang, H., Li, M., Gao, X., Yin, L., Qi, R., Wu, R.S., Chen, X., Ma, Y., Shi, K., et al. (2023). A wearable cardiac ultrasound imager. Nature *613*, 667–675.
5. Zhou, H., Park, J., Lee, Y., Park, J.-M., Kim, J.-H., Kim, J.S., Lee, H.-D., Jo, S.H., Cai, X., Li, L., et al. (2020). Water Passivation of Perovskite Nanocrystals Enables Air-Stable Intrinsically Stretchable Color-Conversion Layers for Stretchable Displays. Adv. Mater. *32*, 2001989.
6. Zheng, Y.-Q., Liu, Y., Zhong, D., Nikzad, S., Liu, S., Yu, Z., Liu, D., Wu, H.-C., Zhu, C., Li, J., et al. (2021). Monolithic optical microlithography of high-density elastic circuits. Science *373*, 88–94.
7. Chu, B., Burnett, W., Chung, J.W., and Bao, Z. (2017). Bring on the body-NET. Nature *549*, 328–330.
8. Zhou, H., Zou, X., Li, H., Li, T., Chen, L., and Cheng, X. (2020). Decreased secretoglobin family 2A member 1expression is associated with poor outcomes in endometrial cancer. Oncol. Lett. *20*, 24.
9. Lee, Y., Zhou, H., and Lee, T.-W. (2018). One-dimensional conjugated polymer nanomaterials for flexible and stretchable electronics. J. Mater. Chem. C *6*, 3538–3550.
10. Lim, K.-G., Han, T.-H., and Lee, T.-W. (2021). Engineering electrodes and metal halide perovskite materials for flexible/stretchable perovskite solar cells and light-emitting diodes. Energy Environ. Sci. *14*, 2009–2035.
11. Lee, Y., Cho, H., Yoon, H., Kang, H., Yoo, H., Zhou, H., Jeong, S., Lee, G. H., Kim, G., Go, G.-T., et al Advancements in Electronic Materials and Devices for Stretchable Displays Adv. Mater. Technol. 2023, 2201067.
12. Zhou, H., and Park, J.-W. (2015). Effect of the crystallinity of indium tin oxide on the charge transfer at the interfaces and the performances of flexible organic light emitting diodes. Phys. Status Solidi A *212*, 414.
13. Zhou, H., and Park, J.-W. (2015). The effects of compressive stress on the performance of organic light-emitting diodes. Org. Electron. *24*, 272–279.
14. Triambulo, R.E., Cheong, H.-G., Zhou, H., Lee, G.-H., and Park, J.-W. (2014). Hybrid-structured indium tin oxide with Ag nanoparticles as crystalline seeds for transparent electrode with enhanced flexibility and its application to organic light emitting diodes. Jpn. J. Appl. Phys. *53*, 05FB13.
15. Zhou, H., and Park, J.-W. (2016). Elucidating the influences of mechanical bending on charge transport at the interfaces of organic light-emitting diodes. Thin Solid Films *619*, 281–287.
16. Han, T.-H., Park, M.-H., Kwon, S.-J., Bae, S.-H., Seo, H.-K., Cho, H., Ahn, J.-H., and Lee, T.-W. (2016). Approaching ultimate flexible organic light-emitting diodes using a graphene anode. NPG Asia Mater. *8*, e303.
17. Lee, J., Han, T.-H., Park, M.-H., Jung, D.Y., Seo, J., Seo, H.-K., Cho, H., Kim, E., Chung, J., Choi, S.-Y., et al. (2016). Synergetic electrode architecture for efficient graphene-based flexible organic light-emitting diodes. Nat. Commun. *7*, 11791.
18. Zhou, H., Han, S.J., Harit, A.K., Kim, D.H., Kim, D.Y., Choi, Y.S., Kwon, H., Kim, K.-N., Go, G.-T., Yun, H.J., et al. (2022). Graphene-Based Intrinsically

Stretchable 2D-Contact Electrodes for Highly Efficient Organic Light-Emitting Diodes. Adv. Mater. *34*, 2270228.

19. Yun, G., Tang, S.-Y., Lu, H., Zhang, S., Dickey, M.D., and Li, W. (2021). Hybrid-Filler Stretchable Conductive Composites: From Fabrication to Application. Small Science *1*, 2000080.
20. Pozarycki, T.A., Hwang, D., Barron, E.J., III, Wilcox, B.T., Tutika, R., and Bartlett, M.D. (2022). Tough Bonding of Liquid Metal-Elastomer Composites for Multifunctional Adhesives. Small *18*, 2203700.
21. Yoon, I.S., Kim, S.H., Oh, Y., Ju, B.-K., and Hong, J.-M. (2020). Ag flake/silicone rubber composite with high stability and stretching speed insensitive resistance via conductive bridge formation. Sci. Rep. *10*, 5036.
22. Kim, D.W., Kong, M., and Jeong, U. (2021). Interface Design for Stretchable Electronic Devices. Adv. Sci. *8*, 2004170.
23. Park, J.Y., Lee, W.J., Kwon, B.-S., Nam, S.-Y., and Choa, S.-H. (2018). Highly stretchable and conductive conductors based on Ag flakes and polyester composites. Microelectron. Eng. *199*, 16–23.
24. Long, X., Yao, J., Cheng, F., Dou, C., and Xia, Y. (2019). Double B←N bridged bipyridine-containing polymer acceptors with enhanced electron mobility for all-polymer solar cells. Mater. Chem. Front. *3*, 70–77.
25. Matsuhisa, N., Kaltenbrunner, M., Yokota, T., Jinno, H., Kuribara, K., Sekitani, T., and Someya, T. (2015). Printable elastic conductors with a high conductivity for electronic textile applications. Nat. Commun. *6*, 7461.
26. Matsuhisa, N., Inoue, D., Zalar, P., Jin, H., Matsuba, Y., Itoh, A., Yokota, T., Hashizume, D., and Someya, T. (2017). Printable elastic conductors by in situ formation of silver nanoparticles from silver flakes. Nat. Mater. *16*, 834–840.
27. Wang, J., Cai, G., Li, S., Gao, D., Xiong, J., and Lee, P.S. (2018). Printable Superelastic Conductors with Extreme Stretchability and Robust Cycling Endurance Enabled by Liquid-Metal Particles. Adv. Mater. *30*, 1706157.
28. Markvicka, E.J., Bartlett, M.D., Huang, X., and Majidi, C. (2018). An autonomously electrically self-healing liquid metal-elastomer composite for robust soft-matter robotics and electronics. Nat. Mater. *17*, 618–624.
29. Veerapandian, S., Jang, W., Seol, J.B., Wang, H., Kong, M., Thiyagarajan, K., Kwak, J., Park, G., Lee, G., Suh, W., et al. (2021). Hydrogen-doped viscoplastic liquid metal microparticles for stretchable printed metal lines. Nat. Mater. *20*, 533–540.
30. Chen, S., Wang, H.-Z., Zhao, R.-Q., Rao, W., and Liu, J. (2020). Liquid Metal Composites. J. Mat. *2*, 1446–1480.
31. Ohm, Y., Pan, C., Ford, M.J., Huang, X., Liao, J., and Majidi, C. (2021). An electrically conductive silver–polyacrylamide–alginate hydrogel composite for soft electronics. Nat. Electron. *4*, 185–192.
32. Kim, S.H., Baek, G.W., Yoon, J., Seo, S., Park, J., Hahm, D., Chang, J.H., Seong, D., Seo, H., Oh, S., et al. (2021). A Bioinspired Stretchable Sensory-Neuromorphic System. Adv. Mater. *33*, 2104690.
33. Wang, T., Liu, Q., Liu, H., Xu, B., and Xu, H. (2022). Printable and Highly Stretchable Viscoelastic Conductors with Kinematically Reconstructed Conductive Pathways. Adv. Mater. *34*, 2202418.
34. Zhao, Y., Ohm, Y., Liao, J., Luo, Y., Cheng, H.-Y., Won, P., Roberts, P., Carneiro, M.R., Islam, M.F., Ahn, J.H., et al. (2023). A self-healing electrically conductive organogel composite. Nat. Electron. *6*, 206–215.
35. Chen, S., Fan, S., Qi, J., Xiong, Z., Qiao, Z., Wu, Z., Yeo, J.C., and Lim, C.T. (2023). Ultrahigh Strain-Insensitive Integrated Hybrid Electronics Using Highly Stretchable Bilayer Liquid Metal Based Conductor. Adv. Mater. *35*, 2208569.
36. Chronakis, I.S., Grapenson, S., and Jakob, A. (2006). Conductive polypyrrole nanofibers via electrospinning: Electrical and morphological properties. Polymer *47*, 1597–1603.
37. Blinova, N.V., Stejskal, J., Trchová, M., and Prokeš, J. (2008). Control of polyaniline conductivity and contact angles by partial protonation. Polym. Int. *57*, 66–69.
38. Kroon, R., Kiefer, D., Stegerer, D., Yu, L., Sommer, M., and Müller, C. (2017). Polar Side Chains Enhance Processability, Electrical Conductivity, and Thermal Stability of a Molecularly p-Doped Polythiophene. Adv. Mater. *29*, 1700930.
39. Bakhshi, A.K., Ladik, J., and Seel, M. (1987). Comparative study of the electronic structure and conduction properties of polypyrrole, polythiophene, and polyfuran and their copolymers. Phys. Rev. B *35*, 704–712.
40. Lang, U., Müller, E., Naujoks, N., and Dual, J. (2009). Microscopical Investigations of PEDOT:PSS Thin Films. Adv. Funct. Mater. *19*, 1215–1220.
41. Matsuhisa, N., Niu, S., O'Neill, S.J.K., Kang, J., Ochiai, Y., Katsumata, T., Wu, H.-C., Ashizawa, M., Wang, G.-J.N., Zhong, D., et al. (2021). High-frequency and intrinsically stretchable polymer diodes. Nature *600*, 246–252.
42. Hosseini, E., Ozhukil Kollath, V., and Karan, K. (2020). The key mechanism of conductivity in PEDOT:PSS thin films exposed by anomalous conduction behaviour upon solvent-doping and sulfuric acid post-treatment. J. Mater. Chem. C *8*, 3982–3990.
43. Kim, N., Kee, S., Lee, S.H., Lee, B.H., Kahng, Y.H., Jo, Y.-R., Kim, B.-J., and Lee, K. (2014). Highly conductive PEDOT:PSS nanofibrils induced by solution-processed crystallization. Adv. Mater. *26*, 2268–2272.
44. Fan, X., Xu, B., Liu, S., Cui, C., Wang, J., and Yan, F. (2016). Transfer-Printed PEDOT:PSS Electrodes Using Mild Acids for High Conductivity and Improved Stability with Application to Flexible Organic Solar Cells. ACS Appl. Mater. Interfaces *8*, 14029–14036.
45. Worfolk, B.J., Andrews, S.C., Park, S., Reinspach, J., Liu, N., Toney, M.F., Mannsfeld, S.C.B., and Bao, Z. (2015). Ultrahigh electrical conductivity in solution-sheared polymeric transparent films. Proc. Natl. Acad. Sci. USA *112*, 14138–14143.
46. Lee, J.H., Jeong, Y.R., Lee, G., Jin, S.W., Lee, Y.H., Hong, S.Y., Park, H., Kim, J.W., Lee, S.-S., and Ha, J.S. (2018). Highly Conductive, Stretchable, and Transparent PEDOT:PSS Electrodes Fabricated with Triblock Copolymer Additives and Acid Treatment. ACS Appl. Mater. Interfaces *10*, 28027–28035.
47. Wang, Y., Zhu, C., Pfattner, R., Yan, H., Jin, L., Chen, S., Molina-Lopez, F., Lissel, F., Liu, J., Rabiah, N.I., et al. (2017). A highly stretchable, transparent, and conductive polymer. Sci. Adv. *3*, e1602076.
48. Teo, M.Y., Kim, N., Kee, S., Kim, B.S., Kim, G., Hong, S., Jung, S., and Lee, K. (2017). Highly Stretchable and Highly Conductive PEDOT:PSS/Ionic Liquid Composite Transparent Electrodes for Solution-Processed Stretchable Electronics. ACS Appl. Mater. Interfaces *9*, 819–826.
49. Jiang, Y., Zhang, Z., Wang, Y.-X., Li, D., Coen, C.-T., Hwaun, E., Chen, G., Wu, H.-C., Zhong, D., Niu, S., et al. (2022). Topological supramolecular network enabled high-conductivity, stretchable organic bioelectronics. Science *375*, 1411–1417.
50. Yu, Z., Niu, X., Liu, Z., and Pei, Q. (2011). Intrinsically Stretchable Polymer Light-Emitting Devices Using Carbon Nanotube-Polymer Composite Electrodes. Adv. Mater. *23*, 3989–3994.
51. Liang, J., Li, L., Niu, X., Yu, Z., and Pei, Q. (2013). Elastomeric polymer light-emitting devices and displays. Nat. Photonics *7*, 817–824.
52. Liang, J., Li, L., Tong, K., Ren, Z., Hu, W., Niu, X., Chen, Y., and Pei, Q. (2014). Silver nanowire percolation network soldered with graphene oxide at room temperature and its application for fully stretchable polymer light-emitting diodes. ACS Nano *8*, 1590–1600.
53. Kim, J.H., and Park, J.W. (2021). Intrinsically stretchable organic light-emitting diodes. Sci. Adv. *7*, eabd9715.
54. Han, T.-H., Lee, Y., Choi, M.-R., Woo, S.-H., Bae, S.-H., Hong, B.H., Ahn, J.-H., and Lee, T.-W. (2012). Extremely efficient flexible organic light-emitting diodes with modified graphene anode. Nat. Photonics *6*, 105–110.
55. Ahn, S., Han, T.-H., Maleski, K., Song, J., Kim, Y.-H., Park, M.-H., Zhou, H., Yoo, S., Gogotsi, Y., and Lee, T.-W. (2020). A 2D Titanium Carbide MXene Flexible Electrode for High-Efficiency Light-Emitting Diodes. Adv. Mater. *32*, 2000919.
56. Zhou, H., Han, S.J., Lee, H.-D., Zhang, D., Anayee, M., Jo, S.H., Gogotsi, Y., and Lee, T.-W. (2022). Overcoming the Limitations of MXene Electrodes for Solution-Processed Optoelectronic Devices. Adv. Mater. *34*, 2206377.

57. Zhou, H., Han, S.J., Harit, A.K., Kim, D.H., Kim, D.Y., Choi, Y.S., Kwon, H., Kim, K.N., Go, G.T., Yun, H.J., et al. (2022). Graphene-Based Intrinsically Stretchable 2D-Contact Electrodes for Highly Efficient Organic Light-Emitting Diodes. Adv. Mater. *34*, 2203040.

58. Dong, J., and Portale, G. (2020). Role of the Processing Solvent on the Electrical Conductivity of PEDOT:PSS. Adv. Mater. Interfac. *7*, 2000641.

59. Zhang, Z., Li, X., Chen, Z., Zhang, Y., Peng, H., Lai, J.-C., Niu, S., Xu, C., Shih, C.-C., Wang, C., et al. (2022). Investigation of Gas-Water-Sand Fluid Resistivity Property as Potential Application for Marine Gas Hydrate Production. Nature *24*, 624.

60. Savagatrup, S., Chan, E., Renteria-Garcia, S.M., Printz, A.D., Zaretski, A.V., O'Connor, T.F., Rodriquez, D., Valle, E., and Lipomi, D.J. (2015). Plasticization of PEDOT:PSS by Common Additives for Mechanically Robust Organic Solar Cells and Wearable Sensors. Adv. Funct. Mater. *25*, 427–436.

61. Xie, Z., Xu, R., Chen, J., Li, C., Bao, Z., Zheng, J., Sun, Q., Li, Y., and Tang, J. (2019). The modified PEDOT:PSS as cathode interfacial layer for scalable organic solar cells. J. Org. Electron. *71*, 143–149.

62. Kim, K.M., Ahn, S., Jang, W., Park, S., Park, O.O., and Wang, D.H. (2018). Work function optimization of vacuum free top-electrode by PEDOT:PSS/PEI interaction for efficient semi-transparent perovskite solar cells. Sol. Energy Mater. Sol. Cells *176*, 435–440.

63. Li, Z., Schonberg, R., Guidugli, L., Johnson, A.K., Arnovitz, S., Yang, S., Scafidi, J., Summar, M.L., Vezina, G., Das, S., et al. (2015). A novel mutation in the promoter of RARS2 causes pontocerebellar hypoplasia in two siblings. J. Hum. Genet. *60*, 363–369.

64. van der Pol, T.P.A., Keene, S.T., Saes, B.W.H., Meskers, S.C.J., Salleo, A., van de Burgt, Y., and Janssen, R.A.J. (2019). The Mechanism of Dedoping PEDOT:PSS by Aliphatic Polyamines. J. Phys. Chem. C *123*, 24328–24337.

65. Wang, B., and Facchetti, A. (2019). Mechanically Flexible Conductors for Stretchable and Wearable E-Skin and E-Textile Devices. Adv. Mater. *31*, 1901408.

66. Xu, F., and Zhu, Y. (2012). Highly conductive and stretchable silver nanowire conductors. Adv. Mater. *24*, 5117–5122.

67. Kwon, S.-J., Han, T.-H., Ko, T.Y., Li, N., Kim, Y., Kim, D.J., Bae, S.-H., Yang, Y., Hong, B.H., Kim, K.S., et al. (2018). Extremely stable graphene electrodes doped with macromolecular acid. Nat. Commun. *9*, 2037.

68. Liu, N., Chortos, A., Lei, T., Jin, L., Kim, T.R., Bae, W.-G., Zhu, C., Wang, S., Pfattner, R., Chen, X., et al. (2017). Ultratransparent and stretchable graphene electrodes. Sci. Adv. *3*, e1700159.

69. Kwon, N.Y., Park, S.H., Lee, Y., Kong, G.D., Chau, H.D., Yoon, H.J., Woo, H.Y., Hoang, M.H., Cho, M.J., and Choi, D.H. (2022). Uniform Silver Nanowire Patterned Electrode on Robust PEN Substrate Using Poly(2-hydroxyethyl methacrylate) Underlayer. ACS Appl. Mater. Interfaces *14*, 34909–34917.

70. Aizawa, N., Pu, Y.-J., Watanabe, M., Chiba, T., Ideta, K., Toyota, N., Igarashi, M., Suzuri, Y., Sasabe, H., and Kido, J. (2014). Solution-processed multilayer small-molecule light-emitting devices with high-efficiency white-light emission. Nat. Commun. *5*, 5756.

71. Han, S.J., Zhou, H., Kwon, H., Woo, S.-J., and Lee, T.-W. (2023). Achieving Low-Voltage Operation of Intrinsically-Stretchable Organic Light-Emitting Diodes. Adv. Funct. Mater.2211150

72. VahidMohammadi, A., Rosen, J., and Gogotsi, Y. (2021). The world of two-dimensional carbides and nitrides (MXenes). Science *372*, eabf1581.